Bioinspiration & Biomimetics

A stability perspective of bio-inspired UAVs performing dynamic soaring optimally

To cite this article before publication: Imran Mir *et al* 2021 *Bioinspir. Biomim.* in press https://doi.org/10.1088/1748-3190/ac1918

A Stability Perspective of Bio-Inspired UAVs Performing Dynamic Soaring Optimally

Imran Mir

Air University, Aerospace & Aviation Campus, Kamra, Pakistan

Sameh A. Eisa

University of Cincinnati, Ohio, USA

Haitham Taha

University of California, Irvine, California, USA

Adnan Maqsood

National University of Sciences & Technology (NUST), Islamabad,Pakistan

Suhail Akhtar

Institute of Space Technology, Islamabad, Pakistan

Tauqeer Ul Islam

Air University, Aerospace & Aviation Campus, Kamra, Pakistan

Dynamic soaring phenomenon, exhibited by soaring birds, has long been a biological inspiration for the aerospace and control engineering communities. If this fascinating phenomenon, which allows soaring birds to perform almost un-powered flights using wind shear, can be mimicked by Unmanned-Aerial-Vehicles (UAVs), then UAVs performance have a substantial potential to enhance technologically and economically as well. Even though there have been considerable amount of research covering the modeling, optimization, control and simulation aspects of different UAVs performing dynamic soaring, there is little to non conclusive work analyzing the stability of such UAVs about the soaring orbits. In this paper, we present a comprehensive framework for determining the stability of soaring UAVs utilizing both linear (Floquet-based) and nonlinear (Contraction-theory-based) techniques. Stability analysis under Floquet remained inconclusive , which provoked nonlinear Contraction formulation in order to reach a conclusive stability assessment for the actual nonlinear fixed-wing UAV performing dynamic soaring. Furthermore, parametric

variation along with numerical simulations were conducted to ascertain the response of the actual nonlinear system when perturbed from its nominal motion studied in this paper. The analysis and simulations revealed that the system posses instability as the UAV motion diverges from its nominal trajectory and follow an undesirable path. By this result, we conclude, for the first time in literature, that UAVs performing dynamic soaring in an optimal way to reduce wind shear requirements, are inherently unstable. The results of this paper suggests that mimicking dynamic soaring by UAVs, require careful investigations of tracking and regulatory controls that should be implemented.

Keywords. Bio-Inspired Flight, Contraction Analysis, Dynamic Soaring, Flight Dynamics, Floquet Analysis, Optimal control, Unmanned Aerial Vehicles.

Nomenclature

Abbreviations

AR	Aspect ratio of the wing
b	Wing span (m)
c	Wing chord (m)
C	Monodromy matrix
C_L	Lift coefficient
C_{L_α}	Lift coefficient variation wrt angle of attack
C_D	Drag coefficient
C_{D_0}	Zero lift drag coefficient
D	Aerodynamic Drag force (N)
e	Oswald efficiency factor
$\boldsymbol{F}$	Generalized Jacobian
$f(x,t)$	Nonlinear function Virtual velocity between flow fields
g	Acceleration due to gravity (m/s^2)
$GPOPS$	**G**eneral **P**urpose **OP**timization **S**oftware
h	Altitude (m)
h_0	Surface correctness factor
h_{ref}	Reference altitude (m)
$\dot{h}$	Rate of change of altitude (m/s)
$\boldsymbol{I}$	Identity matrix
$IPOPT$	**I**nterior **P**oint **OPT**imizer

J	Performance Index
J_S	Symmetric Jacobian
K	Induced drag coefficient
L	Aerodynamic Lift force (N)
$LTIS$	**L**inear **T**ime **I**nvariant **S**ystem
$LTVS$	**L**inear **T**ime **V**arying **S**ystem
$\boldsymbol{M}$	Continuously differentiable symmetric matrix
m	Mass of the vehicle (kg)
n	Load factor
$NTVS$	**N**onLinear **T**ime **V**arying **S**ystem
P	T-periodic matrix
q_∞	Dynamic pressure (Pa)
R	Constant matrix
S	Wing planform area (m^2)
$SNOPT$	**S**parse **N**onlinear **OPT**imizer
t_0	Initial time (s)
t_f	Final time (s)
UAV	Unmanned Aerial Vehicle
V	UAV flight speed (m/s)
$V_{w_{ref}}$	Reference wind velocity (m/s)
V_w	Wind shear velocity (m/s)
$\dot{V}_W$	Rate of change of wind velocity (m/s^2)
x	Position vector along east direction (m)
y	Position vector along north direction (m)
$y(t)$	Time varying solution
z	Transformed state variable

Greek Symbols

α	Angle of attack (°)
β	Positive real number
γ	Flight path angle (°)
θ	Pitch angle (°)

$\mathbf{\Theta}$	Square matrix
ρ	Density of the air (Kg/m^3)
ϕ	Bank angle (°)
ψ	Azimuth angle (°)
Φ_t^A	Fundamental solution matrix
λ_{max}	Largest Eigenvalue
δ	Partial derivative
$\dot{\delta x}$	Virtual velocity between flow fields

I. Introduction

Dynamic soaring is a fascinating flight strategy that utilizes wind gradients to perform long duration flights by harvesting atmospheric energy [1]. The energy needed to perform such a long duration of flight is gained from the wind in the proximity of the surface. In a region of about 20 m above the sea surface, the speed of the horizontal wind changes considerably with the altitude to yield what is known as 'wind shear' [2–4]. By flying across the wind gradient region periodically, energy is harvested from the spatial wind speed distribution. This has been observed amongst birds (albatrosses, eagles, etc.) and offers promise for use in the flight of Unmanned Aerial Vehicles (UAVs) [5]. What is fascinating about this maneuver (see figure 1), is that it enables the soaring birds to travel large distances almost without flapping its wings [6]. The dynamic soaring cycle can be considered to have four characteristic flight phases, namely (a) windward climb, (b) high altitude turn, (c) tailwind descent, and (d) low altitude turn. To start with the maneuver, the UAV mimicking soaring birds goes into the head wind gaining height, trading off kinetic energy with potential energy, and at the highest point takes a steep turn and dives down with tail wind. It continues to descend until it reaches the lowest point trading potential energy for kinetic energy (gain in the velocity) until it reaches the minimum possible height. At that point, it takes the low altitude turn and returns to the original orientation to culminate the energy neutral maneuver cycle.

Nature-inspired flight [2, 4, 5, 7–12], understandingly, attracted many engineering communities because nature could provide inspiring and already proved to function ideas, techniques and designs for man-made technologies [13]. The aeronautical and control engineering communities have been researching if the very powerful dynamic soaring phenomenon can be applied effectively to advance UAVs technology, simply by mimicking the flight of the soaring birds and fly for free in areas where the wind shear is present [14, 15]. It is well established that due to the limitation on the size and weight of UAVs, adding on-board energy sources is very technically-challenging, which limits the range and endurance of these platforms [16] . Therefore,

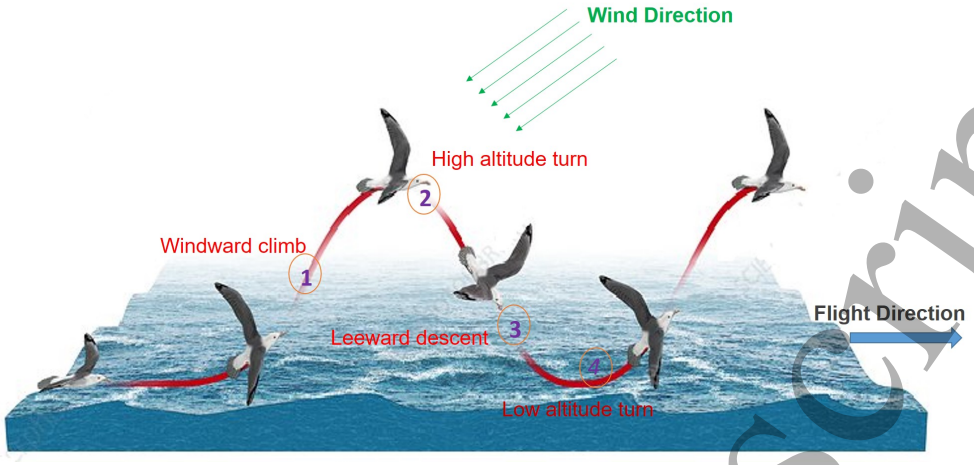

Figure 1: Dynamic soaring maneuver

dynamic soaring application can serve a great deal by reducing the need for having larger on-board engines since the wind shear provides most, if not all, of the power needed for flight.

Not surprising, these potentials of advancing the performance/technology of UAVs by dynamic soaring, attracted researchers to study all kind of technical aspects of dynamic soaring and its application to UAVs. Wharington [17] formulated dynamic soaring trajectories for a UAV utilizing heuristic approach (pitch and bank control) and proposed different approaches for closed-loop design. The heuristics however did not present the methodology to predict speed gain per loop of maneuver [18]. Later, the heuristic control was also found ineffective [19]. Zhao [20] studied the optimal dynamic soaring trajectories for loiter, basic, and travel modes. Dynamic soaring maneuver can be represented by several parameters: maximum altitude, upper and lower speed, and the maneuver duration (cycle period). Several authors studied the effect of these parameters on the energy gain and the minimum required wind shear [10, 17, 21–23]. Sachs and Da Costa [24] performed studies to extend dynamic soaring to full-scale sailplanes. Based upon the values of wind shear conventionally found near mountain ridges, it was considered possible. Gordan [25] carried out detailed search in this regard with an aim to prove or disprove the viability of dynamic soaring for full size aircraft. He showed that full size sailplanes could extract energy from horizontal wind shears, although the utility of the energy extraction could be marginal depending on the flight conditions and type of sailplane used. Recently, koessler [26] configured dynamic soaring trajectory optimization into an optimal control problem, and then presented an online reinforcement learning controller that can execute the DS maneuver to a steady state. The learning controller was taught by a tracking controller that has been shown to achieve steady state dynamic soaring control in simulation under stable and known (to the UAV) environmental conditions. Additionally, the studies [15, 20, 27–30] focused on the flight dynamics, modeling, control, real time simulations involved in the process of UAVs performing dynamic soaring. It is worth mentioning that

actually gliders tried taking advantage from the dynamic soaring phenomenon. RC glider utilizing dynamic soaring that involves performance of oval flight pattern over ridges have succeeded to achieve flight speeds in excess of 545 mph [31]. The rapid growth in the UAVs and motorized gliders market have further boosted the requirement to perform long duration autonomous flights utilizing dynamic soaring apart from conventional energy harvesting techniques such as solar/thermal batteries and static soaring.

In our recent review-work [32], we have discussed the history of biological inspiration by soaring birds and how this inspiration led to the current studies of UAVs performing dynamic soaring. In the same work, we documented how nonlinear modeling of the flight dynamics of UAVs have developed to adopt dynamic soaring. Similarly, numerical optimization/simulation techniques have evolved to provide the tools necessary for studying UAVs performing dynamic soaring in real time. Moreover, we have shown how one can develop an optimal control problem to generate a dynamic soaring trajectory in which energy from wind shear is minimized as well. At the end of our review-work, we identified some challenges to advance dynamic soaring, namely through two tracks of research: 1) Allowing morphologies to the body of the UAV, so it reflects similar behaviors to soaring birds which may provide significant enhancements (addressed in [27]), and 2) Investigating the possibility of nonlinear controllability studies since the fixed-wing UAV problem is highly nonlinear and that the linear control literature of that problem seems incomplete and immature (addressed in [28]). In [28], the entire controllability problem was studied and characterized for fixed-wing UAV performing dynamic soaring. In that paper, it was found that pitch and roll control signals are enough to guarantee controllability along the dynamic soaring, optimal and non-optimal, trajectories. An interesting observation in our study of controllability [28] revealed, that geometric nonlinear controllability analysis is needed for studying the system, not just linear control theory. This is because the UAV with pitch and roll controls (under-actuated system) was shown *nonlinearly controllable* even though the system is *linearly uncontrollable*. Thus, it became apparent that the system has to be always studied from nonlinear theory perspective.

Could it be the case that linear analysis fails to conclude stability as it did with controllability? The literature, to the best of our knowledge, did not have answer to these questions. The only relevant stability work found is by Swaminathan [33, 34], who performed linear stability analysis (based on eigenvalues). The problem of augmenting the stability as 6-DOF and 3-DOF dynamic soaring model was treated from the context of a periodic coefficient system. The eigenvalues and eigenvectors were compared to a 3-DOF system and the mode shapes to level flight and banked turn. A linear time periodic system about this orbit was determined and its stability was studied using only linearized analysis techniques. However, the work did not consider evaluating stability aspects along the trajectory and did not include any nonlinear analysis to verify the reported lower stability margins. There has been no consolidated work reported on determining the

stability of the dynamic soaring periodic orbits and its dependence on system parameters. It is exceptionally important to find out about the stability of the UAV performing dynamic soaring. The trajectories can get disturbed by gusts or crosswinds causing the UAV to veer off-course. Although a dedicated control system can be designed to overcome the perturbations, but an inherently stable orbit can greatly reduce the control effort and power. This is why assessing the stability is of great importance to the control design advancements as well. It is worth emphasizing that the optimized dynamic soaring trajectories, as presented in [32], are time varying. This means that traditional equilibrium-based techniques, such as eigenvalues for linear/linearized systems, simply, cannot be used; This could explain why the dynamic soaring stability problem has been rarely researched in-depth. One now can see that other stability analysis techniques that are mathematically defined for time varying systems, should be investigated to determine if they can be useful to the dynamic soaring problem.

The contribution of this paper is to perform a comprehensive stability analysis along the optimal dynamic soaring trajectory $(\boldsymbol{x}^*, \boldsymbol{u}^*)$, where $\boldsymbol{x}$ is the state space vector and $\boldsymbol{u}$ is the control input vector. Not only that these analyses are the first in literature for the concerned problem under study, they are also utilizing mathematical techniques that can be useful in many other flight dynamics and control studies dealing with nonlinear time varying systems. Moreover, this paper draws a parallelism in its results with the original controllability results we published recently [28]. This should enrich and complete the picture for scholars working on the flight dynamics and control design to enhance/innovate/advance UAV aiming to perform dynamic soaring in an optimal way.

In this paper, we use the well-defined numerical optimization process and flight dynamic modeling we recommended in our review-work [32] to find the dynamic soaring optimal trajectory. Since dynamic soaring loiter maneuver is periodic in nature, the problem of analyzing stability along the trajectory is treated from the context of a periodic coefficient system. To access the stability aspect along the periodic time varying soaring trajectory, both linear (*Floquet theory*) and nonlinear (*Contraction theory*) techniques are utilized for the first time in literature for this system. These methods are chosen as they determine stability characteristics of the system along the optimal trajectory (time-variant) instead of evaluating stability of equilibrium point(s) on the trajectory. The authors of this paper believe that the provided formulation process along with the conducted analysis methodology, are generic strategies for evaluating UAV stability characteristics along optimal soaring trajectories. In other words, the provided framework is extendable to cover different span of flight scenarios, parameter variations and situations that different classes of UAVs can be studied under. Additionally, the proposed methodology is computationally-relevant and independent of particular platform(s). The conclusions and results of the paper have been verified by parametric variations and numerical simulations, all of which support our results.

The structure of this paper is as following: Section II introduces the modeling work used in this paper, along with generating the optimal soaring trajectories that are used in the stability analysis, Sections III and IV represent the major contribution and stability results of this paper, and Section V concludes the paper.

II. Problem Formulation and Generation of Optimal Trajectories

A. UAV model

The UAV utilized in this research has a nominal wingspan of 1.75 m, fuselage length of 1.5 m and 2.1 kg mass (Refer Figure 2). The aerodynamic surfaces are constructed utilizing NACA 2412 aerofoil. Complete details of the UAV model parameters are adopted from [32] and elaborated in table. 1.

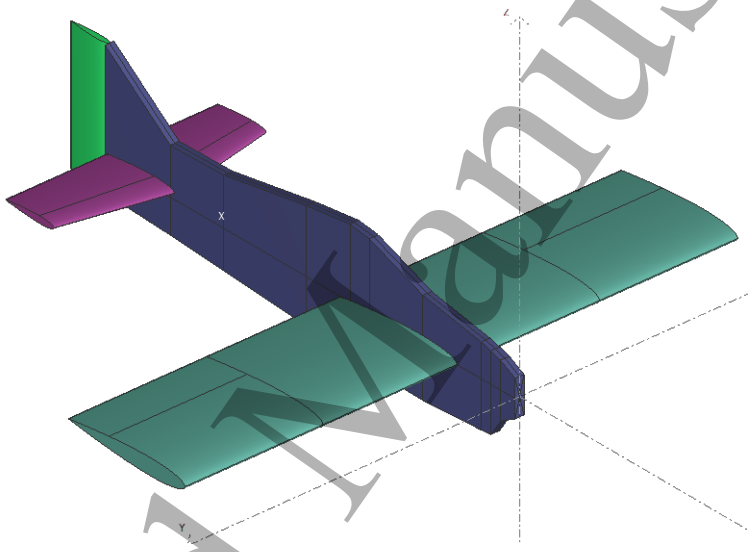

Figure 2: UAV model

No	Parameter	Value	No	Parameter	Value
1	Nominal mass (m)	2.1 Kg	5	Wing chord (c)	0.6 m
2	Fuselage length	1.5 m	6	Fuselage diameter	0.1 m
3	Nominal Wing span (b)	1.55 m	7	Aspect ratio (AR)	2.9
4	Wing area (S)	$1.05\,m^2$	8	Oswald's efficiency factor (e)	0.8

Table 1: UAV model parameters.

B. Wind Shear Modeling

Dynamic soaring is dependent on wind shear which occurs in the boundary layer over any surface. Wind shear involves changes in wind speed and/or direction over a short distance height in the atmosphere, and

can be segregated into different categories, as explained by wharington [17]. The wind shear considered in this research is the vertical variation of the horizontal wind shear, in which the magnitude of the horizontal wind increases with altitude. The strength of wind velocity is virtually zero at sea level and increases with the altitude till its magnitude becomes equal to the boundary layer free stream wind. Majority of the research on UAV energy extraction from wind shear, has been done with strong assumptions on the wind shear models, often as it is the case here, conducted and determined empirically. The logic usually is that given certain geographical and meteorological conditions, the wind shear can be approximated with a wind model of a certain profile after collecting too many data points that can be satisfactory to construct such models/profiles. The mean velocity profile of actual wind gradients can be approximated using empirical models [30, 35–37] utilizing linear or nonlinear wind models (Power or Logarithmic law based).

To approximate wind shear, various empirical models [32] have been used to predict wind profiles over flat terrains (with varying topographies) including linear [25, 30, 35], exponential [37, 38] or logarithmic [23, 27, 28, 39, 40] models. Based on the available models in literature and as we cited properly in the paper, this logarithmic profile is commonly used in meteorological studies and is the most applicable/reliable to measurements near the surface of the earth and over sea [23, 39, 40]. Due to this reason, the logarithmic wind shear profile (refer Figure 3) as represented by Eq. (1) is utilized [23, 27, 40].

$$V_W = V_{w_{ref}} \frac{\ln \frac{h}{h_0}}{\ln \frac{h_{ref}}{h_0}}, \tag{1}$$

where V_w is the wind velocity at altitude h, $V_{w_{ref}}$ is the wind velocity at reference altitude h_{ref} and h_0 is the surface correctness factor.Rate of change of wind velocity with varying altitude is mathematically represented by Eq. (2):

$$\dot{V_W} = \frac{dV_W}{dt} = \frac{dV_W}{dh}.\frac{dh}{dt}, \tag{2}$$

where $\frac{dV_W}{dh}$ is the wind shear parameter. It is the parameter whose value is required to be minimized, such that it is enough to permit sustainable dynamic soaring. Wind shear is the rate of change of wind speed w.r.t altitude (representing the slope of the wind velocity Vs altitude) and has the units (1/sec). This is the least amount of wind shear which is required to exist at sea level condition beyond which UAV would not be able to perform dynamic soaring. This minimum required wind shear is mathematically ascertained by configuring the problem as Optimal control problem and solved numerically utilizing Optimal Control solver GPOPS-II (refer section II C)

From Eq. (1), the wind shear ie $\frac{dV_W}{dh}$ can be computed as

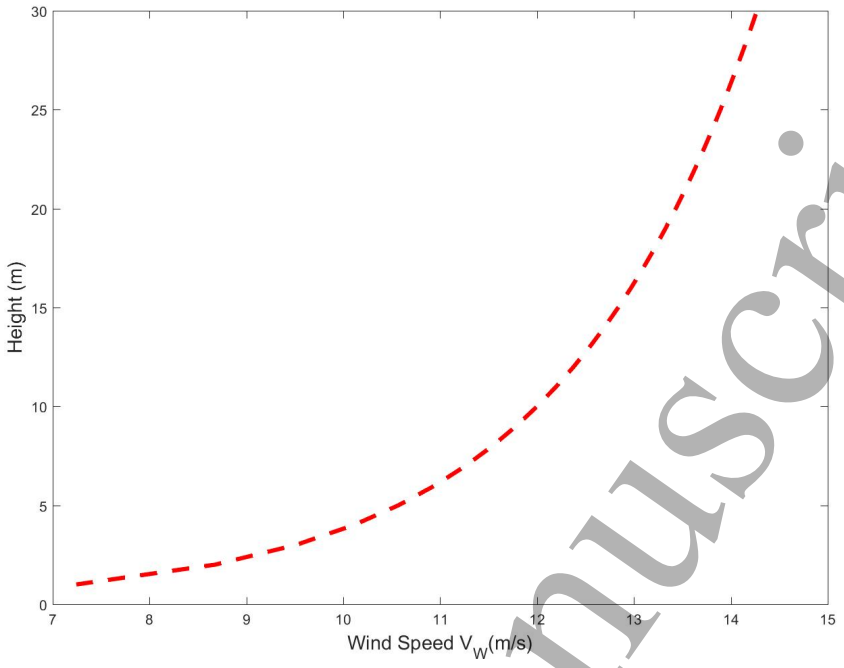

Figure 3: Logarithmic wind profile ($V_{w_{ref}}$=5m/s,h_{ref}=5m,h_0=0.03)

,

$$\frac{dV_W}{dh} = V_{w_{ref}} \frac{1}{h \ln \frac{h_{ref}}{h_0}}. \tag{3}$$

Also $\dot{h} = \frac{dh}{dt}$ is given as

$$\dot{h} = V \sin\gamma. \tag{4}$$

Eq. (2) can be written as

$$\dot{V_W} = V_{w_{ref}} \frac{1}{h \ln \frac{h_{ref}}{h_0}} V \sin\gamma. \tag{5}$$

Also $V_{w_{ref}}$ is the minimum required wind shear that is required to perform sustainable dynamic soaring. Wind shear is the rate of change of wind spped w.r.t altitude (representing the slope of the wind velocity Vs altitude) and has the units (1/sec). This is the least amount of wind shear which is required to exist at sea level condition beyond which UAV would not be able to perform dynamic soaring. This minimum required wind shear is mathematically ascertained by configuring the problem as Optimal control problem and solved numerically utilizing Optimal Control solver GPOPS-II (refer section II C).

C. Flight Dynamics Modeling & Optimization Framework

The optimization framework utilized in this research to generate optimal soaring trajectories is based upon GPOPS-II [41]. This is MATLAB® based framework which utilizes variable-order Gaussian quadrature technique to convert the original continuous-time infinite dimensional optimal control problem into a finite dimensional Nonlinear Programming (NLP) problem. The NLP is then solved utilizing **I**nterior **P**oint **OPT**imizer (IPOPT) or **S**parse **N**onlinear **OPT**imizer (SNOPT).

In this research, UAV dynamics are modeled utilizing a 3D point-mass model [17, 20, 30, 32] which is mathematically represented by Eq. (6). It is worth mentioning that the reader may refer to [32] for more detailed explanation about the modeling process , derivation and assumptions.

$$\begin{aligned}
\dot{V} &= \frac{1}{m}\left[-\boldsymbol{D} - mg\sin\gamma - m\dot{V}_W\cos\gamma\sin\psi\right] \\
\dot{\psi} &= \frac{1}{mV\cos\gamma}[\boldsymbol{L}\sin\phi - m\dot{V}_W\cos\psi] \\
\dot{\gamma} &= \frac{1}{mV}[\boldsymbol{L}\cos\phi - mg\cos\gamma + m\dot{V}_W\sin\psi\sin\gamma] \\
\dot{x} &= V\cos\gamma\sin\psi + V_W \\
\dot{y} &= V\cos\gamma\cos\psi \\
\dot{h} &= V\sin\gamma
\end{aligned} \tag{6}$$

The state $\boldsymbol{x}(t)$ and the control $\boldsymbol{u}(t)$ vectors are defined in Eq. (7) and Eq. (8) respectively.

$$\boldsymbol{x}(t) = [V,\ \psi\ \gamma,\ x,\ y,\ h]^T,\ \ \boldsymbol{x}(t) \in \mathbb{R}^6. \tag{7}$$

$$\boldsymbol{u}(t) = [C_L,\ \phi], \boldsymbol{u} \in \mathbb{R}^2. \tag{8}$$

To implement the loiter maneuver, trajectory optimization problem is transformed to an optimal control problem, that minimizes the performance index (refer Eq. (9), subject to the boundary constraints (refer Eq. (10)) and path constraints (refer Eqs. (11)).

$$J = min\left[V_{w,ref}\right] \tag{9}$$

$$\boldsymbol{x}(t)_{t_f} = \boldsymbol{x}(t)_{t_0} \tag{10}$$

$$V_{min} < V < V_{max}, \psi_{min} < \psi < \psi_{max}, \gamma_{min} < \gamma < \gamma_{max}$$
$$x_{min} < x < x_{max}, y_{min} < y < y_{max}, h \geq 0; \phi_{min} < \phi < \phi_{max} \quad (11)$$

where $V_{w,ref}$ is the minimum required wind shear that still permits dynamic soaring. , t_f and t_o denotes the final and initial times respectively.

The permissible variations for the state and control variables (in defined units) during the maneuver are listed in table. 2.

S No	Parameter	Value	S No	Parameter	Value
1	NonLinear logarithmic wind model parameter	h_{ref} = 10m , h_0= 0.03	6	Max load factor (n)	< 6
2	Cycle time	1 to 40s	7	Permissible variation along east direction	−500m to 500m
3	Permissible azimuth variations	-450° to 450°	8	Permissible variation in north direction	−500m to 500m
4	Permissible velocity variations	5 to 60m/s	9	Permissible altitude range	0 to 500m
5	Permissible fight path angle variation	−70° to 70°	10	Terminal constraints	Final state= Initial state

Table 2: Permissible state and control variations

D. Impact of UAV model Parameter on Soaring Process

The optimal soaring trajectories for UAVs are usually formulated with the objective to determine the minimum wind shear beyond which dynamic soaring will not be possible. This minimum required wind shear is associated with fixed parameters of the system. Finding the required minimum wind shear to perform dynamic soaring posed a challenging numerical problem, because of the coupled nonlinear nature of the equations of motion. The wind shear determined numerically for soaring should be realize-able, i.e. it should be of a magnitude, which normally and practically exists over conventional environments (such as over sea, over hills, rural areas and so on), making dynamic soaring possible over these areas.

A parametric sweep of the parameters of the UAV model used in this paper, namely mass and wing span, was performed to determine the impact of model/parametric variation on soaring process. This was performed to determine the relative impact which these parameters might create on the soaring process and the determination of the minimum wind shear required to perform dynamic soaring. Evaluating these variations of the mass and wing span is quite significant as it also tests which classes of UAVs can actually/practically perform dynamic soaring.

This evaluation is also of another fundamental importance to the context of this research, as stability

perspectives of these soaring orbits will be subsequently analyzed utilizing linear/nonlinear techniques. The numerical optimization process was performed initially for the nominal UAV parameters defined in table. 1 and state/control variables bounds as listed in table. 2. The optimization was then extended to a range of conditions in which certain UAV model parameters such as mass and wing span were varied while the other process variables as listed in table. 1 and table. 2 were kept the same. Table. 3 depicts the results of the different cases evaluated in this sweep.

S No	Mass (Kg)	Span(m)	Minimum required wind shear at sea level (1/s)	S No	UAV Mass (Kg)	Span Value (m)	Minimum required wind shear at sea level (1/s)
1	1.2	1.25	0.1431	13	1.5	1.25	0.1288
2	1.2	1.55	0.1499	14	1.5	1.55	0.1341
3	1.2	1.75	0.1511	15	1.5	1.75	0.1376
4	1.2	1.95	0.1531	16	1.5	1.95	0.1410
5	2.1	1.25	0.1020	17	3.5	1.25	0.0900
6	2.1	1.55	0.1039	18	3.5	1.55	0.0907
7	2.1	1.75	0.1066	19	3.5	1.75	0.0910
8	2.1	1.95	0.1099	20	3.5	1.95	0.0924
9	4.5	1.25	0.0810	21	5.5	1.25	0.0718
10	4.5	1.55	0.0828	22	5.5	1.55	0.0737
11	4.5	1.75	0.0833	23	5.5	1.75	0.0771
12	4.5	1. 95	0.0847	24	5.5	1.95	0.0799

Table 3: Impact of model parameters on optimization process

The impact of UAV mass variation on the system dynamics is catered in 3-DOF modal as elaborated in Eq. (6).The variation of span has an direct impact on both the aerodynamic coefficient (C_L , C_D) as well as the aerodynamic force (Lift and drag). The aerodynamic modal utilized in this research are in accordance with [42, 43] and are represented as follows:-

$$\begin{gathered} S = b * c_{nominal}; AR = b/c_{nominal} \\ e = 1.78 * (1 - 0.045 * AR^{0.68}) - 0.64 \\ C_L = C_{L_0 + C_{L_\alpha}\alpha}; C_D = C_{D_0 + \frac{1}{\pi * e * AR} * {C_L}^2} \\ L = 1/2 * \rho * V^2 * S * C_L; D = 1/2 * \rho * V^2 * S * C_D \end{gathered} \tag{12}$$

It can be evidently seen that for a given mass, the minimum required wind shear value increases as the span increases (see figure 4). Similarly, for a given span, the wind shear requirement increases as the mass decreases. This is understandable from physical sense as well. During the low altitude phase of the the dynamic soaring cycle, the velocity is high and the angle of attack requirement is low. Lower span

helps in improving aerodynamic performance (i.e, low induced drag) and therefore lower required minimum wind shear. Similarly, if the span increases, the induced drag increases and more wind shear is required to overcome that drag and perform energy neutral soaring process. Likewise, the Dynamic Soaring Force (DSF) which acts as propulsive source during the soaring process, is directly dependant upon the mass of the UAV. The magnitude of the force decreases as the mass decreases, stretching the minimum required wind shear to higher values for sustained soaring.

It can be noticed from the results of the mass and the span parametric variation (as shown in table. 3 and figure 4) that the soaring process and framework used in this paper, to obtain the minimum required wind shear and therefore the optimal soaring trajectory associated with it, are in fact extendable to other classes of UAVs.

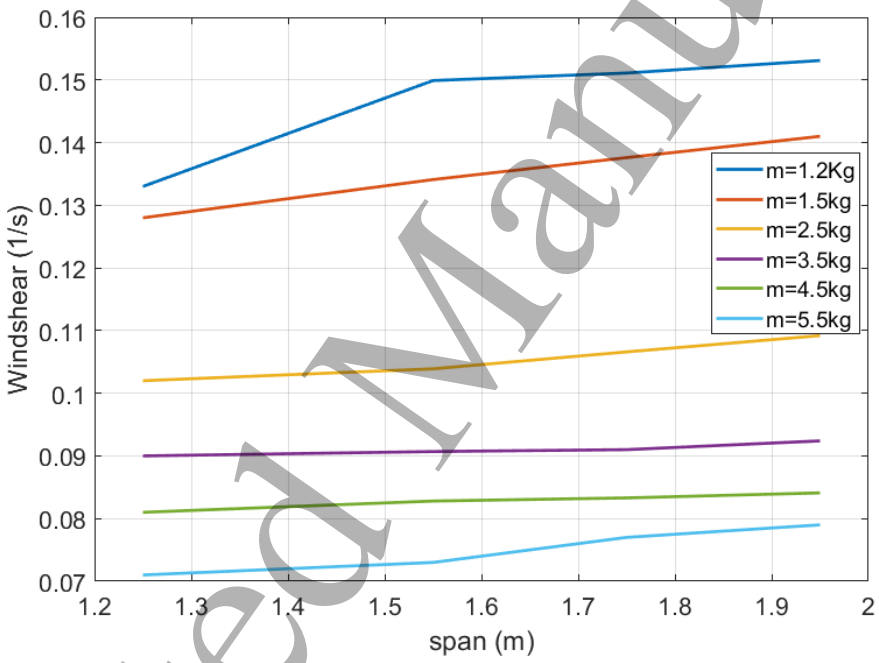

Figure 4: Variation in minimum required wind-shear: Mass and span variations

E. Generation of Optimal Soaring Trajectories for nominal UAV model

The optimal soaring trajectory, for dynamic soaring loiter maneuver for the nominal UAV parameters defined in table. 1 and state/control variables bounds as listed in table. 2, is presented in Fig. 5. The optimized trajectory ensures that energy is being extracted from the wind shear during both wind ward climb and downwind descent phases. This increase in energy is utilized to overcome the energy consumed during the high and low altitude turns (in specific the low altitude turn associated with high flight velocities). It is worth mentioning that the reader may refer to [32] for more detailed explanation and step-by-step process

to generate the optimal soaring trajectory.

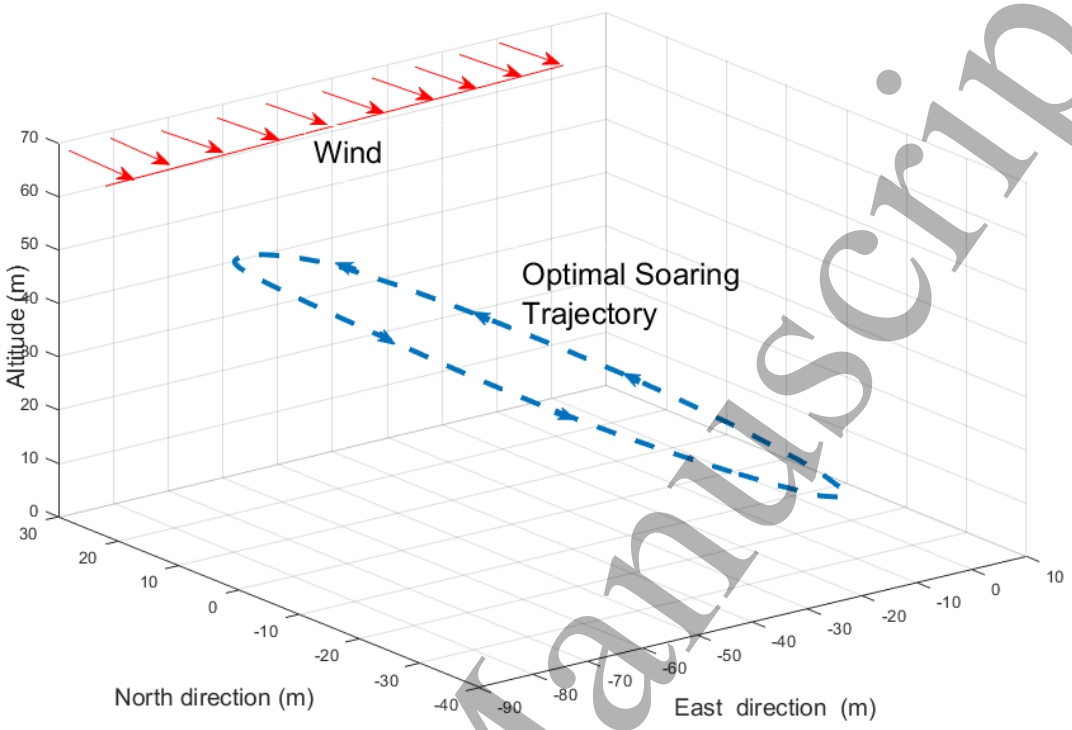

Figure 5: Optimal Loiter trajectory

Similarly, the optimal trajectories for the individual states and the associated optimal control are depicted in Fig. 6. The angle of attack variation allows the provisioning of excess lift in higher altitude regions associated with lower velocities. Similarly the bank angle control ensures that the desired flight path angle and azimuth conditions are met to conform to the energy neutral soaring cycle.

III. Stability Analysis Utilizing Floquet Technique

Having introduced the basics of dynamic soaring and the generation of optimal soaring trajectory for the loiter maneuver (section II), now we perform the stability analysis. In this section, stability analysis along the optimal trajectory $(\boldsymbol{x}^*, \boldsymbol{u}^*)$ (as depicted in Figs. 5 and 6), is performed utilizing Floquet theory. Realizing that the system under study (UAV performing dynamic soaring Eq. (6)), operating with a given $\boldsymbol{u}(t)$, is in the form of Nonlinear-Time-Varying-System (NTVS), it is clear that traditional spectral analyses, such as eigenvalue analysis, will not conclude stability about any point or even a periodic orbit. As a mater of fact, this is true even if all the eigenvalues are with strict negative real part for all t. This has been established by a counter example provided by Markus and Yamabe [44]. Therefore, we turn our attention to *Floquet* method.

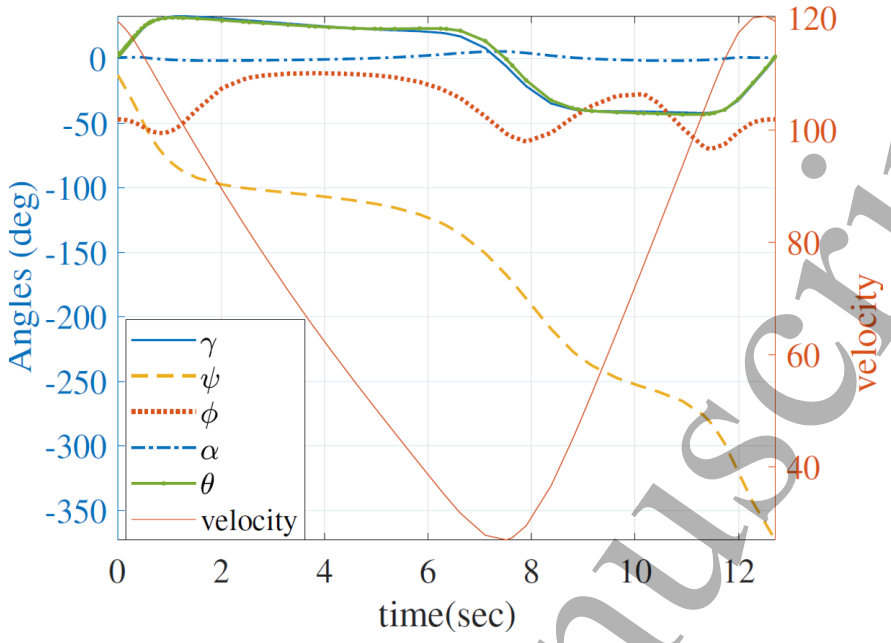

Figure 6: Optimal trajectories for state space and control signals

Floquet analysis is applicable to evaluate the stability of a periodic Linear-Time-Varying-System (LTVS) [45–51] by transforming the periodic-LTVS into that of a Linear-Time-Invariant-System (LTIS). Stability of the system is then determined through spectral/eigenvalue analysis. Loiter maneuver being periodic allows the applicability of Floquet theory for evaluating the stability characteristics of the linearized system along the optimal soaring trajectory. Figure 7 shows the steps followed in our analysis. Also, the reader can refer the recent papers [51–54] that have applied Floquet as part of their stability analysis for applications involving NTVS for bio/bio-inspired systems.

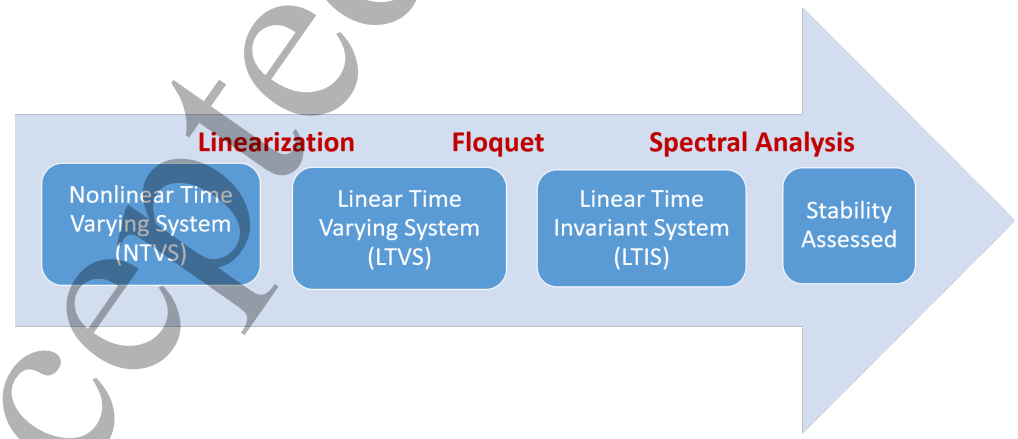

Figure 7: Stability assessment utilizing Floquet

A. Mathematical Framework

Consider the periodic-LTVS,

$$\dot{\mathbf{x}} = \mathbf{A}(t)\,\mathbf{x}, \tag{13}$$

where $\boldsymbol{x} \in \mathbb{R}^n$ with $\mathbf{A} \in \mathbb{R}^{n\times n}$ and T-periodic in t. The flow associated with Eq.(13) can be represented by the so-called *fundamental solution matrix*, written as Eq.(14)

$$\mathbf{\Phi}_t^{\mathbf{A}} = \overrightarrow{\exp}\left(\int_0^t \mathbf{A}(\tau)d\tau\right) \in \mathbb{R}^{n\times n}. \tag{14}$$

The fundamental solution matrix of the system Eq.(13), computed after one period T, is known as the *monodromy matrix* $\mathbf{C} = \mathbf{\Phi}_T^{\mathbf{A}}$.

Theorem 1 ***Linear Floquet Theorem****([55], pg. 11 and [51]). Every fundamental matrix solution* $\mathbf{\Phi}_t^{\mathbf{A}}$ *of the periodic-LTVS* (13) *can be represented as the product* $\mathbf{\Phi}_t^{\mathbf{A}} = \mathbf{P}(t)e^{\mathbf{R}t}$ *of a* T*-periodic matrix (i.e.,* $\mathbf{P}(t) = \mathbf{P}(t+T)$*) and* $\mathbf{R}$ *is a constant matrix given by* $\mathbf{R} = \frac{1}{T}\ln\mathbf{C}$.

Theorem 2 *The system* (13) *is uniformly stable if and only if all Floquet multipliers (eigenvalues of* $\mathbf{C}$*) have moduli less than* 1.

Based on Theorem 1, one can use the transformation $\mathbf{x} = \mathbf{P}\mathbf{y}$ to transform the periodic-LTVS (13) to the LTIS,

$$\dot{\mathbf{y}} = \mathbf{R}\mathbf{y} \tag{15}$$

whose flow after one period is exactly equivalent to the flow of the original periodic-LTVS (13) after one period: $e^{\mathbf{R}T} = \mathbf{\Phi}_T^{\mathbf{A}}$. Then, with $\mathbf{P}(t)$ bounded and $\mathbf{R}$ being a constant matrix, one can compute the eigenvalues to determine stability.

Consider a periodic-NTVS,

$$\dot{\boldsymbol{x}}(t) = \boldsymbol{F}(\boldsymbol{x}, t), \tag{16}$$

where $\boldsymbol{x} \in \mathbb{R}^n$ is the state vector. We can linearize the system (16), so we get a system in the form of (13) in which we can use the results of Theorems 1 and 2 (Floquet method). This can be achieved and applied to the system under study in this paper as shown in figure. 7.

B. Results and Discussion

The nominal UAV model in (6), along with the controls in (8) and its parameters given in table. 1 and table. 2, is used in our stability analysis. This system is periodic-NTVS in nature and we are studying the

stability along the optimal dynamic soaring trajectory $(\boldsymbol{x}^*, \boldsymbol{u}^*)$ characterized in Section II (see Fig. 5). The system under study was numerically integrated to compute the state transition matrix

$$\boldsymbol{\Phi}(t) = \left[\boldsymbol{y}^1(t), \ldots, \boldsymbol{y}^6(t)\right] \left[\boldsymbol{y}_0^1, \ldots, \boldsymbol{y}_0^6\right]^{-1} \tag{17}$$

where $\boldsymbol{y}^1(t), \ldots, \boldsymbol{y}^6(t)$ are the time varying solutions to the independent initial conditions $\boldsymbol{y}_0^1, \ldots, \boldsymbol{y}_0^6$.

The *Monodromy matrix* was ascertained utilizing Eq. (18)

$$\boldsymbol{C} = \boldsymbol{\Phi}(T) = \begin{bmatrix} y^1(T) & y^2(T) & \ldots & y^6(T) \end{bmatrix} \tag{18}$$

Having the *Monodromy matrix constructed*, the Floquet multipliers of the *Monodromy matrix* were determined. The analysis revealed that the periodic solution is *Non-hyperbolic* in nature, as three of the Floquet multipliers lie exactly on the unit disc and three inside the unit circle, as shown in Fig. 8.

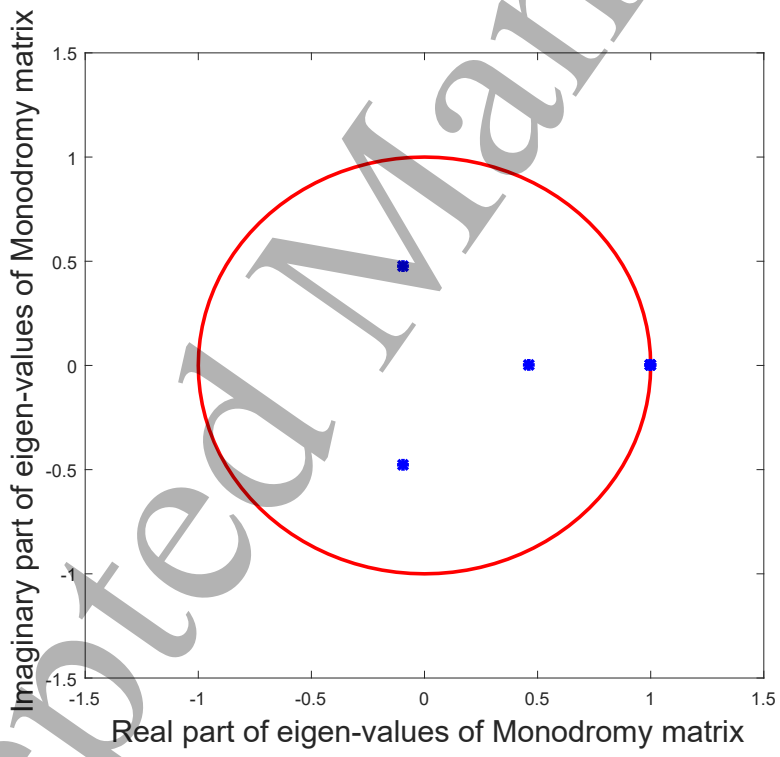

Figure 8: Eigenvalues of the Monodromy matrix

The stability analysis of the system is inconclusive since multiple of Floquet multipliers are on the unit circle. It is also worth mentioning that, since none of the Floquet multipliers lies outside the unit circle, the system could not be considered as unstable with assurance [45]. This result emphasizes the necessity of performing further studies which utilizes nonlinear analysis tools to evaluate stability. It is **remarkably** interesting that linear analysis for the UAV under study is inconclusive under the powerful Floquet method.

This, in a way, draws a parallelism to our controllability results in [28], where the Lie algebraic structure of the system makes nonlinear analysis a must!

C. Expanding the Stability Analysis

Now that the stability analysis along the soaring orbit was performed for the nominal UAV model parameters, it remains to test if the stability assessment would change with different scenarios. In another word, we should test if the inconclusive assessment of stability through linear analysis still hold with different scenarios other than the case we used in our analysis for the nominal UAV parameters. This is significantly important for showing that our stability results can be extended to a range of parameters other than the nominal values. As we have shown in table. 3, the process to generate the dynamic soaring optimal trajectory holds with different combinations of the mass and span, and hence, one can determine the minimum required wind shear that is the main characteristic associated with such optimized trajectories. As one would expect, the stability analysis conducted with the nominal UAV parameters holds with different variations similar to those of table. 3.

Since the minimum wind shear is the most important characteristic/parameter of a given soaring orbit, we decided to expand our stability analysis in that direction. In order to furnish the applicability of the process formulated in this section, a different scenario was simulated to asses stability or otherwise of the UAV. The minimum required wind shear parameter as determined during the optimization process was utilized to reflect the available wind shear. We simulated different scenarios in which the strength of the wind shear available is greater than what is actually needed to perform energy neutral soaring cycles. It is evident from Fig. 9, that the stability results ascertained earlier are still valid. Three of the Eigenvalues of the Monodromy Matrix still remaining on the unit circle, however, the location of the other three eigenvalues which are within the unit circle shifts a bit. They move closer to the unit circle. The stability results and, more importantly, the methodology formulated in this paper are still valid for diversions from the actual conditions for different variations/scenarios.

IV. Stability Analysis Utilizing Contraction Theory

Having analyzed the stability perspectives utilizing linear analysis tools, next we extend the analysis to nonlinear domain. In this section, we perform the stability analysis utilizing nonlinear Contraction analysis technique [56–58]. The use of contraction analysis in this study is motivated by the fact that this technique can be applied directly to the original nonlinear system unlike majority of the other techniques (such as nonlinear Lypnov and linear eigenvalue analysis) which utilize linearized approximations and assess stability of equilibrium point(s). Also it does not require the information of what the nominal motion of the system

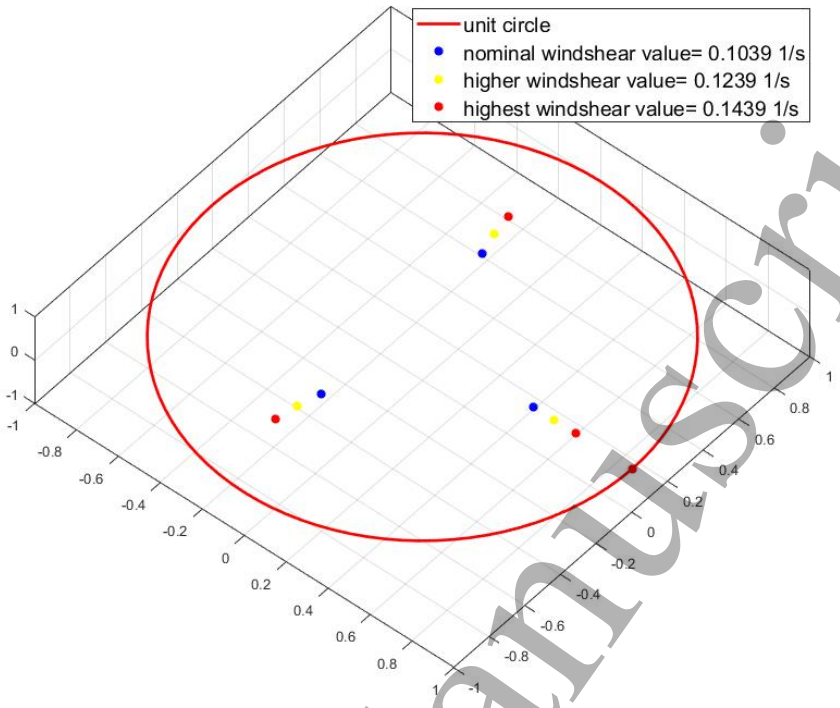

Figure 9: Eigenvalues migration of the perturbed Monodromy matrix

is. The system is stable in the contraction region, where the final behavior of the system is independent of initial perturbations, employing convergence of all perturbed trajectories to the nominal trajectory. Realizing that the fixed-wing UAV problem under study possessed a Lie algebraic structure which required differential geometrical analysis [28] and that linear analysis fails to give information regarding stability (see section III), one finds it tempting to pursue/investigate nonlinear stability analysis; there is a possibility of some parallelism between the present stability analysis and the conducted controllability one [28] in the sense that linear analyses seem to fail and nonlinear analyses seem to be necessary. An advantage of Contraction theory is that it concludes a kind of stability that is associated with trajectories independent on initial conditions, which is useful given the application of the system under study.

A. Mathematical Framework

Consider a general nonlinear system

$$\dot{\boldsymbol{x}} = \boldsymbol{f}(\boldsymbol{x}, t), \tag{19}$$

where $f \in \mathbb{R}^{n\times 1}$ is the nonlinear function and $x \in \mathbb{R}^{n\times 1}$ represents the state. The dynamical system represented by (19) can be imagined as a fluid flow with $\dot{\boldsymbol{x}}$ and $\boldsymbol{x}$ as velocity and position vectors respectively

at time t. The exact differential relation is given by (20)

$$\dot{\boldsymbol{\delta x}} = \frac{\boldsymbol{\delta f}(\boldsymbol{x}, t)}{\boldsymbol{\delta x}} \boldsymbol{\delta x}, \tag{20}$$

where $\boldsymbol{\delta x}$ is a virtual displacement.

Next consider two neighboring trajectories in the flow field defined by Eq.(20). with $\boldsymbol{\delta x}$ being the virtual displacement between them (Fig. 10). The associated quadratic tangent form [59] is defined by Eq. (21)

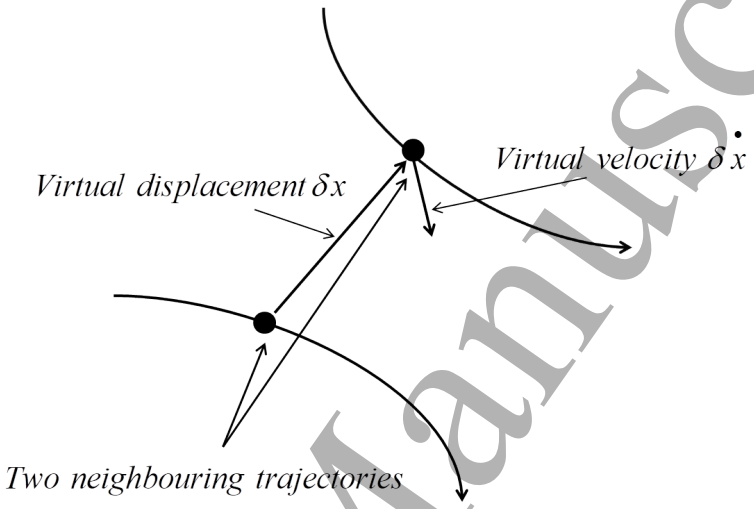

Figure 10: Path flow of two nearby perturbed trajectories

$$\frac{d}{dt}\left(\boldsymbol{\delta x}^T \boldsymbol{\delta x}\right) = 2\left(\boldsymbol{\delta x}^T\right)\left(\delta \dot{\boldsymbol{x}}\right) = 2\boldsymbol{\delta x}^T \frac{\partial f}{\boldsymbol{\partial x}} \boldsymbol{\delta x}. \tag{21}$$

Let us assume $\lambda_{max}(\boldsymbol{x}, t)$ to be the largest eigenvalue of the symmetric Jacobian $\boldsymbol{J}_s$ defined by

$$\boldsymbol{J}_s = \frac{1}{2}\left(\frac{\partial \boldsymbol{f}}{\partial \boldsymbol{x}} + \frac{\partial \boldsymbol{f}}{\partial \boldsymbol{x}}^T\right). \tag{22}$$

Convergence of virtual displacement vector $\delta \boldsymbol{x}$ to 0 is associated with regions having uniformly negative definite Jacobian. This is defined [58] by

$$\exists\, \beta > 0,\, \forall \boldsymbol{x},\, \forall t \geq 0 \;\text{ such that }\; \lambda_{max}(\boldsymbol{x}, t) \leq -\beta \mathbf{I} < 0, \tag{23}$$

where $\mathbf{I}$ is the identity matrix. Then, by using (21) we have

$$\frac{d}{dt}\left(\boldsymbol{\delta x}^T \boldsymbol{\delta x}\right) \leq 2\lambda_{max} \boldsymbol{\delta x}^T \boldsymbol{\delta x}, \tag{24}$$

and hence

$$\|\boldsymbol{\delta x}\| \leq \|\boldsymbol{\delta x_0}\| \, e^{\int_0^t \lambda_{max}(\boldsymbol{x},t)dt}. \tag{25}$$

Now if $\lambda_{max}(x,t)$ is uniformly strictly negative, then from (25), $\|\delta \boldsymbol{x}\|$ converges exponentially to zero irrespective of the initial condition $\boldsymbol{\delta x_0}$. This motivates the following definition.

Definition 1 *[58]: Given system dynamics (19), a contraction region exist in the state space manifold if the associated Jacobian defined by (23) is uniformly negative definite in that region.*

The displacement vector $\delta \boldsymbol{x}$ can alternatively be expressed by a transformation defined by

$$\delta \boldsymbol{z} = \boldsymbol{\Theta} \delta \boldsymbol{x}, \tag{26}$$

where $\boldsymbol{\Theta}(\boldsymbol{x},t)$ is a square matrix. The associated quadratic norm is represented by

$$\begin{aligned} \delta \boldsymbol{z}^T \delta \boldsymbol{z} &= \delta \boldsymbol{x}^T \boldsymbol{\Theta}^T \boldsymbol{\Theta} \delta \boldsymbol{x} \\ \delta \boldsymbol{z}^T \delta \boldsymbol{z} &= \delta \boldsymbol{x}^T \mathbf{M} \delta \boldsymbol{x}, \end{aligned} \tag{27}$$

where $\mathbf{M}$ is a continuously differentiable symmetric matrix [60]. In general Eq. (26) is not integrable which employees that new coordinates $\boldsymbol{z}(\boldsymbol{x},t)$ may not be found but δz and $\delta \boldsymbol{z}^T \delta \boldsymbol{z}$ can always be defined. This requires $\mathbf{M}$ to be uniformly positive definite, so that the exponential convergence of

$$\delta z \to 0 \implies \delta x \to 0 \tag{28}$$

Using (26), time-derivative of $\delta \boldsymbol{z} = \boldsymbol{\Theta} \delta \boldsymbol{x}$ and $\delta \boldsymbol{x} = \boldsymbol{\Theta}^{-1} \delta \boldsymbol{z}$, is given as

$$\frac{d}{dt}\left(\delta \boldsymbol{z}\right) = \boldsymbol{F} \delta \boldsymbol{z}, \tag{29}$$

where $\boldsymbol{F} = \left(\dot{\boldsymbol{\Theta}} \boldsymbol{\Theta}^{-1} + \boldsymbol{\Theta} \frac{\delta \boldsymbol{f}}{\delta \boldsymbol{x}} \boldsymbol{\Theta}^{-1}\right)$ is the generalized Jacobian in $\delta \boldsymbol{z}$ coordinates [60]. The associated quadratic norm is

$$\frac{d}{dt}(\delta \boldsymbol{z}^T \delta \boldsymbol{z}) = 2 \delta \boldsymbol{z}^T \frac{d}{dt}\left(\delta \boldsymbol{z}\right) = 2 \delta \boldsymbol{z}^T \boldsymbol{F} \delta \boldsymbol{z} \tag{30}$$

Exponential convergence of $\delta \boldsymbol{z}$ (equivalently $\delta \boldsymbol{x}$) to 0 is associated in regions with uniformly negative definite $\boldsymbol{F}$.

In terms of $\delta \boldsymbol{x}$, Eq. (29) can be written as

$$\boldsymbol{\Theta}^T \frac{d}{dt}\left(\delta \boldsymbol{z}\right) = \mathbf{M} \delta \dot{\boldsymbol{x}} + \boldsymbol{\Theta}^T \dot{\boldsymbol{\Theta}} \delta \boldsymbol{x} = \left(\mathbf{M} \frac{\partial \boldsymbol{f}}{\partial x} + \boldsymbol{\Theta}^T \dot{\boldsymbol{\Theta}}\right) \delta \boldsymbol{x}, \tag{31}$$

with $\mathbf{M} = \mathbf{\Theta}^T\mathbf{\Theta}$ being a symmetric positive definite matrix, exponential convergence of $\delta\boldsymbol{z}$ to 0 implies exponential convergence of $\delta\boldsymbol{x}$ to 0. Time rate of change is represented by

$$\frac{d}{dt}\left(\delta\boldsymbol{x}^T\mathbf{M}\delta\boldsymbol{x}\right) = \delta\boldsymbol{x}^T\left(\frac{\partial\boldsymbol{f}}{\partial\boldsymbol{x}}^T\mathbf{M} + \dot{\mathbf{M}} + \mathbf{M}\frac{\partial\boldsymbol{f}}{\partial\boldsymbol{x}}.\right)\delta\boldsymbol{x}. \tag{32}$$

Exponential convergence of perturbed nearby trajectories to the nominal trajectory can therefore be concluded in regions having uniformly negative $\left(\frac{\partial\boldsymbol{f}}{\partial\boldsymbol{x}}^T\mathbf{M} + \dot{\mathbf{M}} + \mathbf{M}\frac{\partial\boldsymbol{f}}{\partial\boldsymbol{x}}\right)$.

B. Results and Discussion

The UAV periodic-NTVS model in (6), along with the controls in (8), is used in our stability analysis. Stability along the optimal soaring trajectory $(\boldsymbol{x}^*, \boldsymbol{u}^*)$ characterized in Section II (see Fig. 5), requires the system under study to satisfy the trigonometric equality defined in Eq. (32), which will ensure

$$\|\boldsymbol{x}\| \leq \|\boldsymbol{x_0}\|\, e^{\int_0^t \lambda_{max}(\boldsymbol{x},t)dt}. \tag{33}$$

Stability required $\lambda_{max}(x,t)$ of $\left(\frac{\partial\boldsymbol{f}}{\partial\boldsymbol{x}}^T\mathbf{M} + \dot{\mathbf{M}} + \mathbf{M}\frac{\partial\boldsymbol{f}}{\partial\boldsymbol{x}}\right)$ to be uniformly strictly negative as defined in Eq. (23). The contraction formulation was invoked for the nonlinear system in terms of virtual dynamics relationships, i.e. $\partial\boldsymbol{z} = \mathbf{\Theta}\partial\boldsymbol{x}$. Using $\mathbf{\Theta} = \mathbf{M} = \mathbf{I}_{6\times6}$. The eigenvalues of $\left(\frac{\partial\boldsymbol{f}}{\partial\boldsymbol{x}}^T\mathbf{M} + \dot{\mathbf{M}} + \mathbf{M}\frac{\partial\boldsymbol{f}}{\partial\boldsymbol{x}}\right)$ along the optimal trajectory were then determined. The functions of the eigenvalues of the nonlinear system are plotted in Fig. 11.

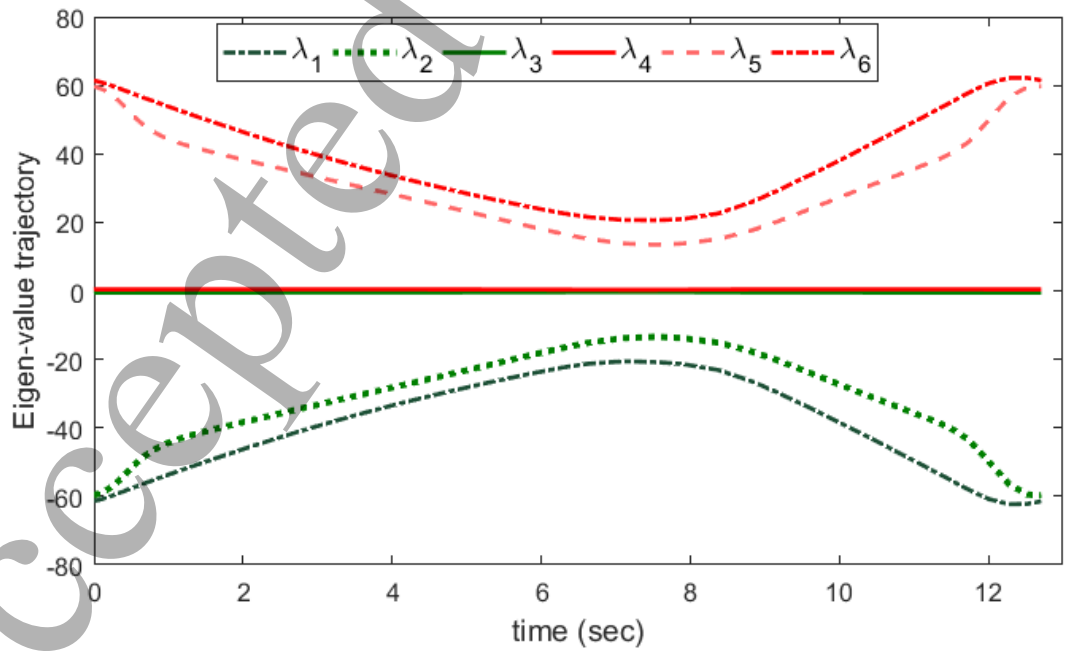

Figure 11: "Symmetric jacobian eigenvalue evolution"

It can be observed in Fig. 11 that eigenvalues λ_4, λ_5 and λ_6 associated with the $\left(\frac{\partial \boldsymbol{f}}{\partial \boldsymbol{x}}^T \mathbf{M} + \dot{\mathbf{M}} + \mathbf{M}\frac{\partial \boldsymbol{f}}{\partial \boldsymbol{x}}\right)$ were not strictly negative due which the nonlinear system during the dynamic soaring maneuver exhibits an unstable response. Numerical simulations performed to ascertain the response of the actual nonlinear system when perturbed from its nominal motion (ψ perterbation) reflects an unstable response. This is evident from Fig. 12, where the UAV motion diverges from its nominal trajectory and follow an undesirable path. The individual response of the individual states of the nonlinear system are depicted in Fig. 13. This unstable phenomena verifies the conclusion drawn from the contraction analysis.

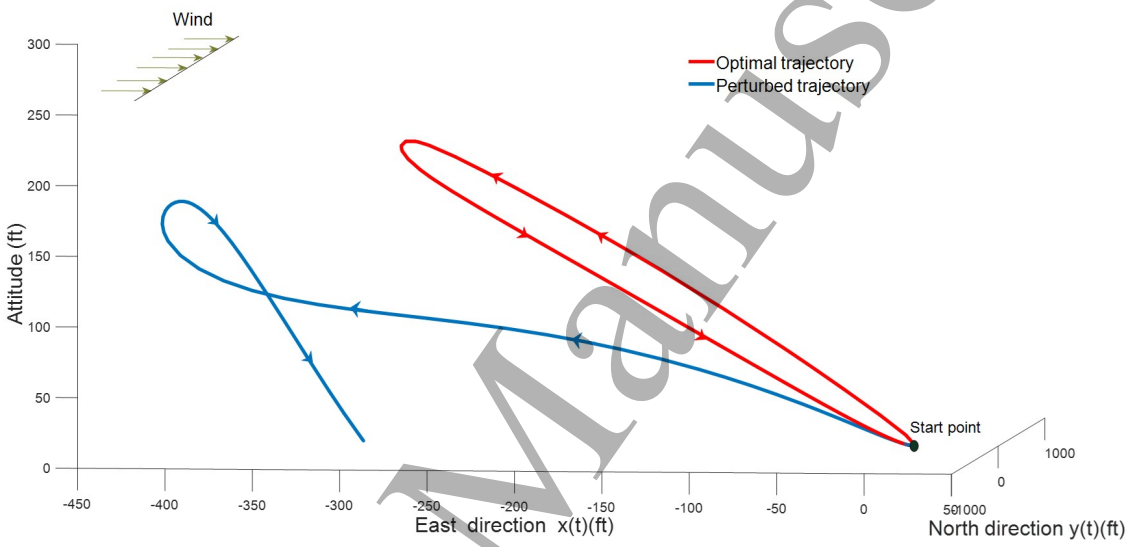

Figure 12: Numerical simulation for perturbed trajectory

By this result, we conclude, for the first time in literature to the best of our knowledge, that similar configuration UAV dynamic soaring optimally to reduce wind shear requirements, are inherently **unstable**. This provokes that dynamic soaring requires a control strategy that can overcome the instability possessed by the system. One direction of developing such controllers can be by trying to construct a stable closed-loop type one, which should not only provide stabilizability to the system, but can be tuned to perform tracking and regulatory functions as well. The controllability results we provided in [28] conclude that the pitch and roll angles (signals) are enough to guarantee full controllability over the UAV performing dynamic soaring. However, nonlinear controllability as defined in [28] does not imply stabilizability. Building on that and adding the results of this paper, it is suggested that the closed-loop controller will be handling the pitch and roll angles based on tracking the optimal soaring trajectory. It is also possible to consider providing the pitch and roll signals, generated in this paper when we constructed the optimal control problem, as reference signals to the controller. Additionally, as a future work, we can study both the stability derivative of the system analyzed in this paper along with the lie brackets provided controllability in [28] to have a more

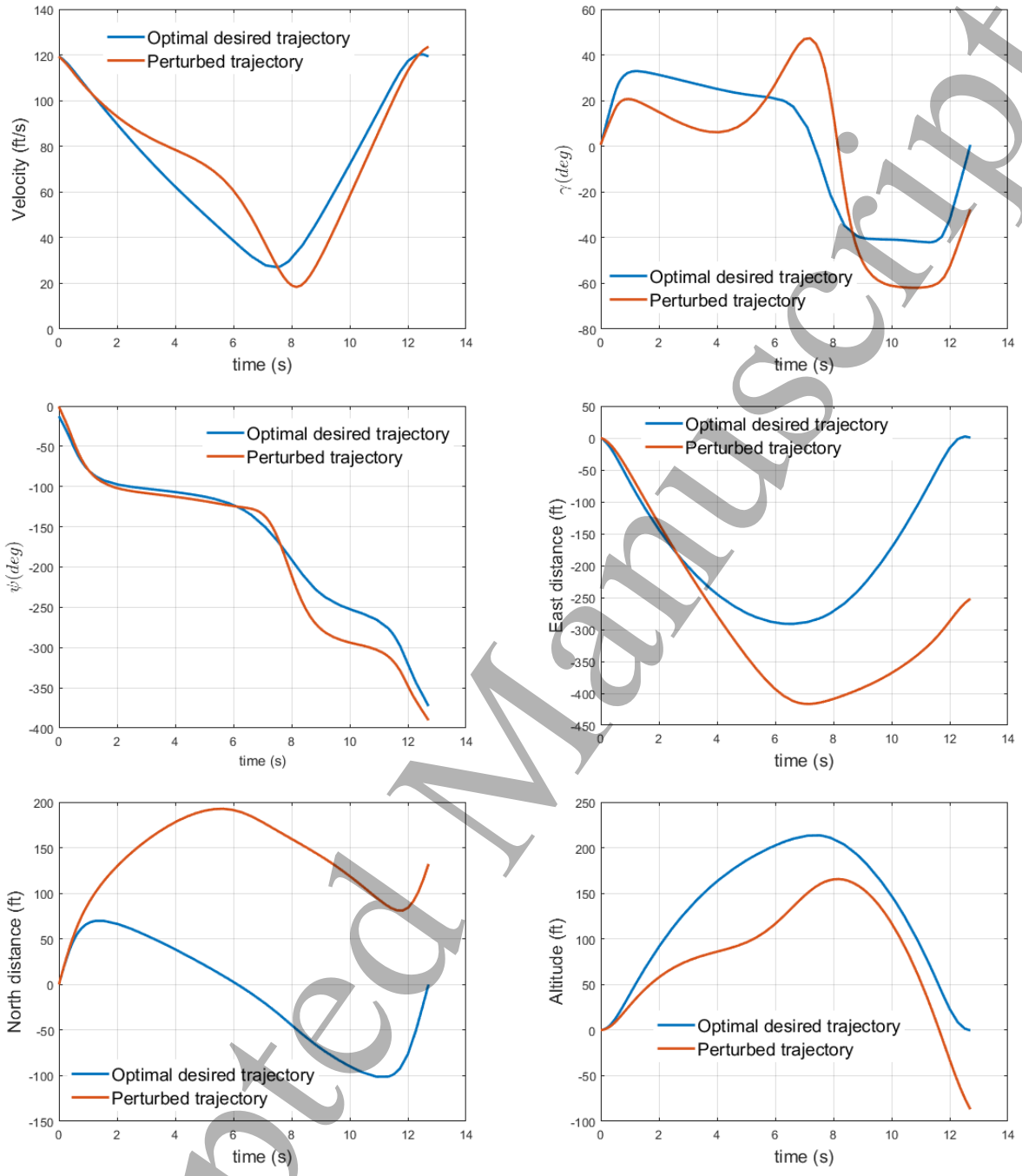

Figure 13: Numerical simulation results for perturbed states

rigorous determination for the specifics/parameters of designing a stable closed-loop type controller, or even other types of tracking and regulatory controllers, to make sure the UAV stays consistently on track and can practically perform the soaring process.

C. Expanding the Stability Analysis

Similar to the analysis performed in sectionIIIC, the stability analysis utilizing contraction analysis along the soaring orbit is tested under a different scenario. This is performed with an aim to see if the stability analysis results vary in case the environmental conditions change. In order to furnish the applicability of the process, another scenario in which the wind shear parameter was different than the minimum required wind shear ascertained through optimization process was utilized. The contraction analysis results as depicted in Figure. 14, clearly demonstrates that that eigenvalues λ_4, λ_5 and λ_6 associated with the $\left(\frac{\partial \boldsymbol{f}}{\partial \boldsymbol{x}}^T \mathbf{M} + \dot{\mathbf{M}} + \mathbf{M}\frac{\partial \boldsymbol{f}}{\partial \boldsymbol{x}}\right)$ were still not strictly negative due which the nonlinear system during the dynamic soaring maneuver exhibits an unstable response. Numerical simulations performed to ascertain the response of the actual nonlinear system when perturbed from its nominal motion (ψ perturbation) still reflects an unstable response. This unstable phenomena verifies the conclusion drawn from the contraction analysis. This clearly demonstrates that the stability results and, more importantly, the methodology formulated in this paper are still valid for diversions from the actual conditions in a spectrum of variations/scenarios.

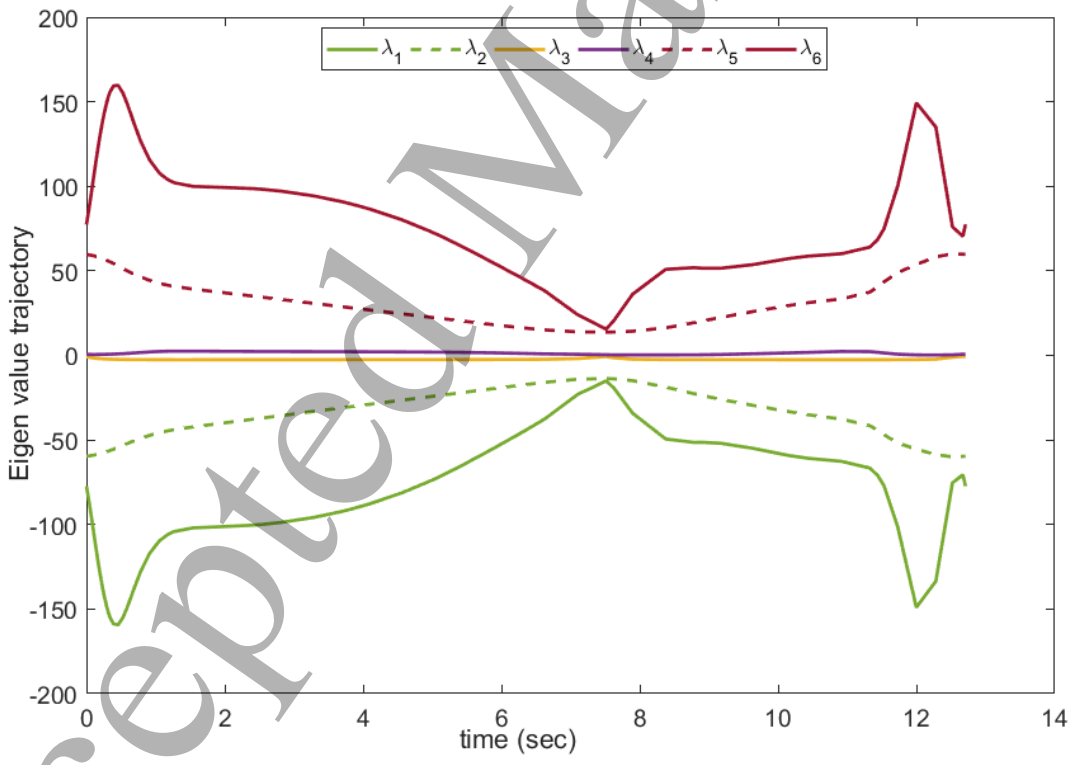

Figure 14: "Symmetric jacobian eigenvalue evolution of system with different wind shear parameter"

V. Conclusion

In this paper, we provided a problem formulation for an UAV set to perform dynamic soaring. Then, we introduced an optimal control problem in which an optimal trajectory was found to minimize the wind shear requirement for the soaring maneuver. The soaring process provided in this paper has also been shown to be valid for different classes of UAVs with a range of masses and wing spans. For a nominal UAV performing optimized dynamic soaring, we provided a stability analysis, that we think is the first of its kind in literature, to asses stability about the optimal trajectory. The analysis revealed a parallelism with our controllability work [28] as we needed to use nonlinear stability theory (Contraction theory) because the linear stability theory (Floquet) is inconclusive. The system is unstable according to contraction theory, even though the system is nonlinearly controllable according to our previous work [28]. Having the system controllable but inherently unstable, as also demonstrated by simulations, means that any proposed control design has to have great deal of trajectory tracking and correction to sustain the flight. The stability results given in this paper has been tested for different wind shear conditions to expand the range of conditions and parametric variations, under which the stability assessment still holds.

Conflict of Interest

The authors of this paper have no conflict of interest to declare.

References

[1] Gao, C. and Liu, H. H., "Dubins path-based dynamic soaring trajectory planning and tracking control in a gradient wind field," *Optimal Control Applications and Methods*, Vol. 38, No. 2, 2017, pp. 147–166.

[2] Denny, M., "Dynamic soaring: aerodynamics for albatrosses," *European Journal of Physics*, Vol. 30, No. 1, 2008, pp. 75.

[3] Sachs, G., Traugott, J., Nesterova, A., and Bonadonna, F., "Experimental verification of dynamic soaring in albatrosses," *Journal of Experimental Biology*, Vol. 216, No. 22, 2013, pp. 4222–4232.

[4] Pennycuick, C., "The flight of petrels and albatrosses (Procellariiformes), observed in South Georgia and its vicinity," *Philosophical Transactions of the Royal Society of London B: Biological Sciences*, Vol. 300, No. 1098, 1982, pp. 75–106.

[5] Wilson, J., "Sweeping flight and soaring by albatrosses," *Nature*, Vol. 257, No. 5524, 1975, pp. 307–308.

[6] Richardson, P. L., "How do albatrosses fly around the world without flapping their wings?" *Progress in Oceanography*, Vol. 88, No. 1, 2011, pp. 46–58.

[7] Cone Jr, C. D. et al., "A mathematical analysis of the dynamic soaring flight of the albatross with ecological interpretations," 1964.

[8] Wood, C., "The flight of albatrosses (a computer simulation)," *Ibis*, Vol. 115, No. 2, 1973, pp. 244–256.

[9] Boslough, M. B., "Autonomous dynamic soaring platform for distributed mobile sensor arrays," *Sandia National Laboratories, Sandia National Laboratories, Tech. Rep. SAND2002-1896*, 2002.

[10] Richardson, P. L., "Upwind dynamic soaring of albatrosses and UAVs," *Progress in Oceanography*, Vol. 130, 2015, pp. 146–156.

[11] Sachs, G. and Grüter, B., "Dynamic Soaring- Kinetic Energy and Inertial Speed," *AIAA Atmospheric Flight Mechanics Conference*, No. 2017-1862, 2017.

[12] Lentink, D. and Biewener, A. A., "Nature-inspired flight beyond the leap," *Bioinspiration & biomimetics*, Vol. 5, No. 4, 2010, pp. 040201.

[13] Taha, H. E., Kiani, M., Hedrick, T. L., and Greeter, J. S., "Vibrational control: A hidden stabilization mechanism in insect flight," *Science Robotics*, Vol. 5, No. 46, 2020, pp. eabb1502–eabb1502.

[14] Hassanalian, M., Throneberry, G., Ali, M., Ayed, S. B., and Abdelkefi, A., "Role of wing color and seasonal changes in ambient temperature and solar irradiation on predicted flight efficiency of the Albatross," *Journal of Thermal Biology*, Vol. 71, 2018, pp. 112–122.

[15] Barate, R., Doncieux, S., and Meyer, J.-A., "Design of a bio-inspired controller for dynamic soaring in a simulated unmanned aerial vehicle," *Bioinspiration & biomimetics*, Vol. 1, No. 3, 2006, pp. 76.

[16] Hassanalian, M. and Abdelkefi, A., "Classifications, applications, and design challenges of drones: A review," *Progress in Aerospace Sciences*, Vol. 91, 2017, pp. 99–131.

[17] Wharington, J. M., "Heuristic control of dynamic soaring," *Control Conference, 2004. 5th Asian*, Vol. 2, IEEE, 2004, pp. 714–722.

[18] Ariff, O. and Go, T., "Waypoint navigation of small-scale UAV incorporating dynamic soaring," *The journal of navigation*, Vol. 64, No. 1, 2011, pp. 29–44.

[19] Lawrance, N. R. and Sukkarieh, S., "A guidance and control strategy for dynamic soaring with a gliding UAV," *Robotics and Automation, 2009. ICRA'09. IEEE International Conference on*, IEEE, 2009, pp. 3632–3637.

[20] Zhao, Y. J., "Optimal patterns of glider dynamic soaring," *Optimal control applications and methods*, Vol. 25, No. 2, 2004, pp. 67–89.

[21] Lawrance, N., Acevedo, J., Chung, J., Nguyen, J., Wilson, D., and Sukkarieh, S., "Long endurance autonomous flight for unmanned aerial vehicles," *AerospaceLab*, , No. 8, 2014, pp. p–1.

[22] Akhtar, N., "Control system development for autonomous soaring," 2010.

[23] Sukumar, P. P. and Selig, M. S., "Dynamic soaring of sailplanes over open fields," *Journal of Aircraft*, 2013.

[24] Sachs, G. and da Costa, O., "Optimization of dynamic soaring at ridges," *AIAA Atmospheric flight mechanics conference and exhibit*, 2003, pp. 11–14.

[25] Gordon, R. J., "Optimal dynamic soaring for full size sailplanes," Tech. rep., Air force institute of tech wright-patterson AFB OH department of aeronautics and astronautics, 2006.

[26] Koessler, J. H., "Towards the Unification of Static and Dynamic Soaring," *AIAA Scitech 2019 Forum*, 2019, p. 0266.

[27] Mir, I., Maqsood, A., Eisa, S. A., Taha, H., and Akhtar, S., "Optimal morphing–augmented dynamic soaring maneuvers for unmanned air vehicle capable of span and sweep morphologies," *Aerospace Science and Technology*, Vol. 79, 2018, pp. 17–36.

[28] Mir, I., Taha, H., Eisa, S. A., and Maqsood, A., "A controllability perspective of dynamic soaring," *Nonlinear Dynamics*, Vol. 93, 2018, pp. 1–16.

[29] Mir, I., Maqsood, A., and Akhtar, S., "Optimization of Dynamic Soaring Maneuvers for a Morphing Capable UAV," *AIAA Information Systems-AIAA Infotech@ Aerospace*, 2017, p. 0678.

[30] Zhao, Y. J. and Qi, Y. C., "Minimum fuel powered dynamic soaring of unmanned aerial vehicles utilizing wind gradients," *Optimal control applications and methods*, Vol. 25, No. 5, 2004, pp. 211–233.

[31] "DSKinetic Kernel Description," http://www.dskinetic.com/, Accessed: 2019.

[32] Mir, I., Eisa, S. A., and Maqsood, A., "Review of dynamic soaring: technical aspects, nonlinear modeling perspectives and future directions," *Nonlinear Dynamics*, 2018, pp. 1–28.

[33] Swaminathan, B. and Mohan, R., "On The Stability of Dynamic Soaring Orbits of UAVs," *2018 Atmospheric Flight Mechanics Conference*, 2018, p. 2832.

[34] Swaminathan, B. and Mohan, R., "Stability and Stability Augmentation of Dynamic Soaring Orbits," *AIAA Aviation 2019 Forum*, 2019, p. 2819.

[35] Akhtar, N., Whidborne, J. F., and Cooke, A. K., "Wind shear energy extraction using dynamic soaring techniques," *American Institute of Aeronautics and Astronautics, AIAA*, Vol. 734, 2009.

[36] Fırtın, E., Güler, Ö., and Akdağ, S. A., "Investigation of wind shear coefficients and their effect on electrical energy generation," *Applied Energy*, Vol. 88, No. 11, 2011, pp. 4097–4105.

[37] Shen, X., Zhu, X., and Du, Z., "Wind turbine aerodynamics and loads control in wind shear flow," *Energy*, Vol. 36, No. 3, 2011, pp. 1424–1434.

[38] Deittert, M., Richards, A., Toomer, C., and Pipe, A., "Dynamic soaring flight in turbulence," *AIAA Guidance, Navigation and Control Conference, Chicago, Illinois*, 2009, pp. 2–5.

[39] Liu, D.-N., Hou, Z.-X., Guo, Z., Yang, X.-X., and Gao, X.-Z., "Bio-inspired energy-harvesting mechanisms and patterns of dynamic soaring," *Bioinspiration & biomimetics*, Vol. 12, No. 1, 2017, pp. 016014.

[40] Sachs, G., "Minimum shear wind strength required for dynamic soaring of albatrosses," *Ibis*, Vol. 147, No. 1, 2005, pp. 1–10.

[41] Patterson, M. A. and Rao, A. V., "GPOPS-II: A MATLAB software for solving multiple-phase optimal control problems using hp-adaptive Gaussian quadrature collocation methods and sparse nonlinear programming," *ACM Transactions on Mathematical Software (TOMS)*, Vol. 41, No. 1, 2014, pp. 1.

[42] Raymer, D. P., "Aircraft design: a conceptual approach (AIAA Education Series)," *Reston, Virginia*, 2012.

[43] Niţă, M. and Scholz, D., *Estimating the Oswald factor from basic aircraft geometrical parameters*, Deutsche Gesellschaft für Luft-und Raumfahrt-Lilienthal-Oberth eV, 2012.

[44] Markus, L. and Yamabe, H., "Global stability criteria for differential systems," *Osaka Mathematical Journal*, Vol. 12, No. 2, 1960, pp. 305–317.

[45] Nayfeh, A. H. and Balachandran, B., *Applied nonlinear dynamics: analytical, computational, and experimental methods*, John Wiley & Sons, 2008.

[46] Brockett, R. W. et al., "Asymptotic stability and feedback stabilization," *Differential geometric control theory*, Vol. 27, No. 1, 1983, pp. 181–191.

[47] Sussmann, H. J. et al., "Subanalytic sets and feedback control," *J. Differential Equations*, Vol. 31, No. 1, 1979, pp. 31–52.

[48] Coron, J.-M., "A necessary condition for feedback stabilization," *Systems & Control Letters*, Vol. 14, No. 3, 1990, pp. 227–232.

[49] Kawski, M., "Stabilization of nonlinear systems in the plane," *Systems & Control Letters*, Vol. 12, No. 2, 1989, pp. 169–175.

[50] Orsi, R., Praly, L., and Mareels, I., "Necessary conditions for stability and attractivity of continuous systems," *International Journal of Control*, Vol. 76, No. 11, 2003, pp. 1070–1077.

[51] Maggia, M., Eisa, S. A., and Taha, H. E., "On higher-order averaging of time-periodic systems: reconciliation of two averaging techniques," *Nonlinear Dynamics*, 2019, pp. 1–24.

[52] Hassan, A. M. and Taha, H. E., "Higher-order averaging analysis of the nonlinear time-periodic dynamics of hovering insects/flapping-wing micro-air-vehicles," *2016 IEEE 55th Conference on Decision and Control (CDC)*, IEEE, 2016, pp. 7477–7482.

[53] Hassan, A. M. and Taha, H. E., "A combined averaging-shooting approach for the trim analysis of hovering insects/flapping-wing micro-air-vehicles," *AIAA Guidance, Navigation, and Control Conference*, 2017, p. 1734.

[54] Taha, H. E., Tahmasian, S., Woolsey, C. A., Nayfeh, A. H., and Hajj, M. R., "The need for higher-order averaging in the stability analysis of hovering, flapping-wing flight," *Bioinspiration & biomimetics*, Vol. 10, No. 1, 2015, pp. 016002.

[55] Hale, J., "Ordinary Differential Equations," 1969.

[56] Lohmiller, W. and Slotine, J.-J., "Control system design for mechanical systems using contraction theory," *IEEE Transactions on Automatic Control*, Vol. 45, No. 5, 2000, pp. 984–989.

[57] Lohmiller, W. and Slotine, J.-J. E., "Nonlinear process control using contraction theory," *AIChE journal*, Vol. 46, No. 3, 2000, pp. 588–596.

[58] Lohmiller, W. and Slotine, J.-J. E., "On contraction analysis for non-linear systems," *Automatica*, Vol. 34, No. 6, 1998, pp. 683–696.

[59] Arnold, V., "Mathematical methods of classical physics," *Graduate Texts in Mathematics*, Vol. 60, 1978.

[60] Lovelock, D. and Rund, H., *Tensors, differential forms, and variational principles*, Courier Corporation, 1989.